Available online at www.sciencedirect.com

SCIENCE DIRECT®

Bioelectrochemistry 64 (2004) 39–45

Bioelectrochemistry

www.elsevier.com/locate/bioelechem

Modelling the internal field distribution in human erythrocytes exposed to MW radiation

J.L. Sebastián*, S. Muñoz San Martín, M. Sancho, J.M. Miranda

Dpt. Física Aplicada III, Facultad de Físicas, Universidad Complutense de Madrid, 28040 Madrid, Spain

Received 18 September 2003; received in revised form 8 December 2003; accepted 5 February 2004
Available online 15 April 2004

Abstract

This paper studies the internal electric field distribution in human erythrocytes exposed to MW radiation. For this purpose, an erythrocyte cell model is exposed to linearly polarized electromagnetic (EM) plane waves of frequency 900 MHz and the electric field within the cell is calculated by using a finite element (FE) technique with adaptive meshing. The results obtained show the dependence of the induced electric field distribution on the main modelling parameters, i.e., the electrical properties (permittivity and conductivity) of the membrane and cytoplasm and the orientation of the cell with respect to the applied field. It is found that for certain orientations, the field amplification within the membrane of the erythrocyte shape cell can be higher than the one observed in an equivalent simple spheroidal geometry cell, commonly used in bioelectromagnetism. The present work shows that a better insight of the interaction of electromagnetic fields with basic biological structures is obtained when the most possible realistic cell shape is used.

Keywords: Erythrocyte; Bioelectromagnetism; Membrane cell; Dosimetry

1. Introduction

Exposure of a biological cell to MW fields can produce a variety of profound biochemical and biophysical responses. Weak electric field effects have generally been attributed, at least as a primary event, to field interaction with either membrane or glycocalix constituents. The magnitude of transmembrane voltage and the deposited energy are basic issues [1,2] for understanding the relation between the exposition to fields and the subsequent physiological reactions at the cell level. Considering that the membrane is a site of high field amplification, it is uncertain how the detailed geometry and electrical properties of the cell can affect the exactness of the predictions in the electric behaviour. Therefore, in order to determine the mechanism of the basic interaction of MW fields with a biological structure, the knowledge of the electric field distribution within the cell membrane is of primary importance.

The cell internal field strength distribution can be directly obtained by solving Laplace equation, and many researchers have used models of cells based on shelled spheres or spheroids that provide simple analytical solutions for a variety of applications (cell manipulation and EM field microdosimetry studies) [3,4]. However, this analytical approach has severe limitations since an explicit solution of Laplace equation requires a geometry consisting in one or several uniform media separated by interfaces which coincide with a surface of a constant coordinate, within a certain set of coordinate types. This excludes other possible geometric configurations such as cylinders or rods. Even for spheroids, this kind of constraining requires the surface of the membrane to be confocal with the main spheroid, producing a non-uniform membrane thickness [5]. Therefore, it turns out that only numerical methods can give a sufficiently precise estimation of field values in realistic cell anatomies. However, conventional computational methods have difficulties in dealing with a very thin membrane in a shelled structure, and it is for this reason that up to now, geometric configurations representing more realistic cell shapes, such as erythrocytes have not been considered.

* Corresponding author. Tel.: +34-91-394-43-93; fax: +34-91-394-51-96.
E-mail address: jlsf@fis.ucm.es (J.L. Sebastián).

1567-5394/$ - see front matter © 2004 Elsevier B.V. All rights reserved.
doi:10.1016/j.bioelechem.2004.02.003

Detailed numerical calculations of the electric field within a mammalian cell with basic spherical, cylindrical and spheroidal geometries have been already carried out by the authors [6,7] in previous works. Using a finite element (FE) technique, it was shown that the electric field induced in the membrane and cytoplasm of a spherical shape cell model was lower than the value found in spheroidal and cylindrical geometries, especially when complex cell structures that included bound water layers for the membrane and cytoplasm were considered. The results indicated the important role played by the geometry of the cell model in the electric field determination. These studies made also clear that in order to have a good insight into the possible mechanisms of the action of electromagnetic fields, including athermal effects, more realistic models than cylindrical and spheroidal geometries should be used. These more precise shapes would in turn, require highly refined calculation techniques with considerably higher computing times.

In this paper, we have focused our interest in the interaction of a linearly polarized electromagnetic (EM) plane wave that impinges on erythrocytes, the biggest cell population in blood. For this, the electric field distribution inside the uniform thickness membrane and cytoplasm is numerically calculated. The frequency of the MW radiation used in this work is 900 MHz and both orientations of the E field (electric and magnetic polarizations) with respect to the cell model have been considered. This frequency is extensively used in industrial and scientific applications such as drying, hardening, defrosting, etc., and in some countries. it is still used as the carrier frequency by cellular phones and wireless surveillance systems [8]. The numerical technique used to calculate the field distribution is based on the well-known finite elements (FE) theory. However, the efficiency and precision of this technique have been improved by using perfectly matched layers (PML) in the boundary conditions of the radiation region and an adaptive mesh in the mesh sizes for the different cell layers.

2. Cell model and numerical method

The erythrocyte was considered as a biconcave structure with major semiaxes $a = b = 3.75$ μm and a minor semiaxis $c = 1.5$ μm, as shown in Fig. 1. The shape of the biconcave erythrocyte was generated from the Cassini oval represented by the relation

$$(x^2 + y^2 + \xi_1^2)^2 - 4\xi_1^2 x^2 = \xi_2^4 \quad (1)$$

where ξ_1 and ξ_2 are shape parameters [9,10]. The 3D cell shape is obtained through rotation of the Cassini oval around the y axis. Parameterization and coordinate transformation equations were derived using Mathematica [11,12]. A uniform shell is generated by shifting the Cassini surface a constant distance d along the normal at each point x, y. The values of the volume and surface of the Cassini generated shape are 118 μm^3 and 129 μm^2, respectively. These values are comparable to the values found in the literature.

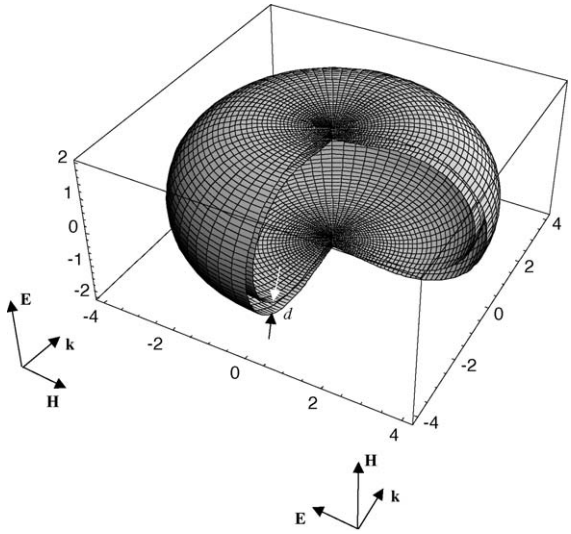

Fig. 1. Geometrical model of the shelled erythrocyte. The quarter section cut shows the constant thickness membrane and the cytoplasm of the cell. In order to appreciate the membrane, its thickness has been exaggerated. Both orientations of the cell, with the external E field parallel to the minor and major axes, are considered.

The cell is formed by two media: the membrane and the cytoplasm. The membrane is represented by a shell with constant thickness of $d = 8$ nm that has a very low conductivity and a frequency-independent relative permittivity [13]. The cytoplasm is a physiological saline solution with a protein volume fraction of 0.26. The cell is immersed in an external continuous medium (the radiation region) formed by an electrolyte with the dielectric properties of physiological saline.

In order to study the influence of the electrical properties on the internal field distribution, the relative permittivities of both membrane and cytoplasm were varied from 2 to 20 and from 30 to 70, respectively. Similarly, the membrane conductivity was varied from 0 to 12 mS/m. A typical value for the cytoplasm conductivity is 0.5 S/m [14–16]. However, the effect of molecular dispersions can produce significant variations of cytoplasm permittivity and conductivity in the frequency range close to 1 GHz [17] and for this reason, the cytoplasm conductivity was varied from 0.3 to 1.2 S/m. These ranges of values are typical of a cell structure and have been used in the literature. The values for the permittivity and conductivity of the external medium are 71.8 and 1.95 S/m, respectively. The permittivity value has been extrapolated from low frequencies taking into account the dielectric dispersion of bound and free water [18].

The cell is exposed to a linearly polarized electromagnetic plane wave propagating along the y-axis with E

field component along the major or the minor axis of the erythrocyte with an intensity of $E = 1$ V/m, as shown in Fig. 1.

3. Numerical method

In this paper, a finite element (FE) technique [19] has been used to determine the electric field intensity within the different layers of the cell. The full Maxwell equations are solved considering a discretization of the geometry into tetrahedral elements. Due to the fact that the dimensions involved in the different parts of the cell structure vary in several orders of magnitude (nanometers for the membrane compared with microns for the cytoplasm), in order to obtain an accurate result for the E intensity within the different regions, an adaptive mesh is used so that the density of tetrahedra in the membrane region had to be considerably higher ($N \sim 10{,}000$) than the corresponding number for the region occupied by the cytoplasm ($N \sim 8000$). In order to keep the computational resource requirements reasonable, the computational domain is truncated to a radiation region (external medium) in which the cell is immersed and surrounded by perfectly matched layers (PML). This provides a reflectionless interface between the region of interest and the PML layers at all incident angles [20]. The dimensions of the radiation region (of the order of four wavelengths in the external medium) are adjusted so that a good compromise between accuracy and reasonable computing time is obtained. The electric field value at points inside each tetrahedron is interpolated from the values at the vertices of the tetrahedron. To obtain a precise description of the field, the region occupied by each tetrahedron must be small enough for the field to be interpolated from the nodal values. The accuracy of this technique is conditioned by the smallest size of the mesh single element.

The resulting matrix equation for the field values at the mesh nodes is solved by an iterative method and a solution is found when a convergence criterion limit is accomplished. In all analysis, the convergence error limit was smaller than 10^{-6} for a result to be considered correct and the computing times for 2-GHz speed microprocessor were of the order of 240 min.

In the analysis, the orientation of the cell model exposed to MW was varied so both situations have been considered; when the electric vector is aligned with the minor axis and with the major axis.

4. Analysis of the results

Table 1 shows the magnitude of the induced electric field in V/m within the different layers of the cell structure for the parameters listed on the first column. The values show that a significant amplification of the electric field is produced within the membrane. The amplification factor found for the erythrocyte shape depends significantly on the orientation of the cell with respect to the external field; when E field is applied along the minor axis the electric field intensities within the membrane and cytoplasm are significantly higher than those obtained when the external E field is parallel to the major axis. The field in the external medium (1 V/m), even at short distances, is practically unaffected by the cell polarization.

Table 1
Electric field distribution within the membrane and cytoplasm of a realistic and oblate spheroid models of an erythrocyte

Electrical Parameters	Erythrocyte		Oblate spheroid	
$\varepsilon_{mem} = 9$ $\sigma_{mem} = 0$ $\varepsilon_{cyto} = 50$ $\sigma_{cyto} = 1$ S/m				
$E_{membrane}$ (V/m)	7.48	4.91	6.60	6.0
$E_{cytoplasm}$ (V/m)	1.50	1.10	1.20	1.08

The values are calculated along the E field direction for both orientations of the cell model. The external field intensity is 1 V/m.

To analyze the sensitivity of these results to changes in electrical properties of the membrane, its relative permittivity and conductivity were varied from 2 to 22 and from 0 to 12 mS/m, respectively. Fig. 2 shows the amplitude of the electric field distribution within the cell membrane as a function of its relative permittivity. For these results, the membrane conductivity has been kept equal to zero at the working frequency used in this work [13]. The electric field is shown along the minor and major axes. As it can be observed, the electric field intensity is significantly reduced as the value of the membrane relative permittivity increases. The conductivity of the membrane is typically very low, and its influence on the electric field within the membrane is less significant than that of the permittivity. When the membrane conductivity varied from 0 to 12 mS/m, and for a fixed permittivity value of 9, the maxima variations of the electric field observed within the membrane were found to be less than 5% and 3% for the external field applied parallel to the minor and major axes respectively. It is also observed that the membrane electric field values obtained when the external field is along the minor axis are higher than those obtained when the field is applied along the major axis.

In order to analyze the influence of changes in electrical properties of the cytoplasm on the E field within the membrane, its permittivity and conductivity were varied from 30 to 70 and from 0.3 to 1.2 S/m, respectively. Fig. 3 shows the influence of the cytoplasm permittivity on the membrane electric field, keeping constant the rest of the cell parameters. Higher values for the electric field within the membrane are found as the cytoplasm permittivity is increased. In contrast, cytoplasm conductivity variations have less influence on the electric field within the membrane. When the cytoplasm conductivity was varied from 0.3 to 1.2

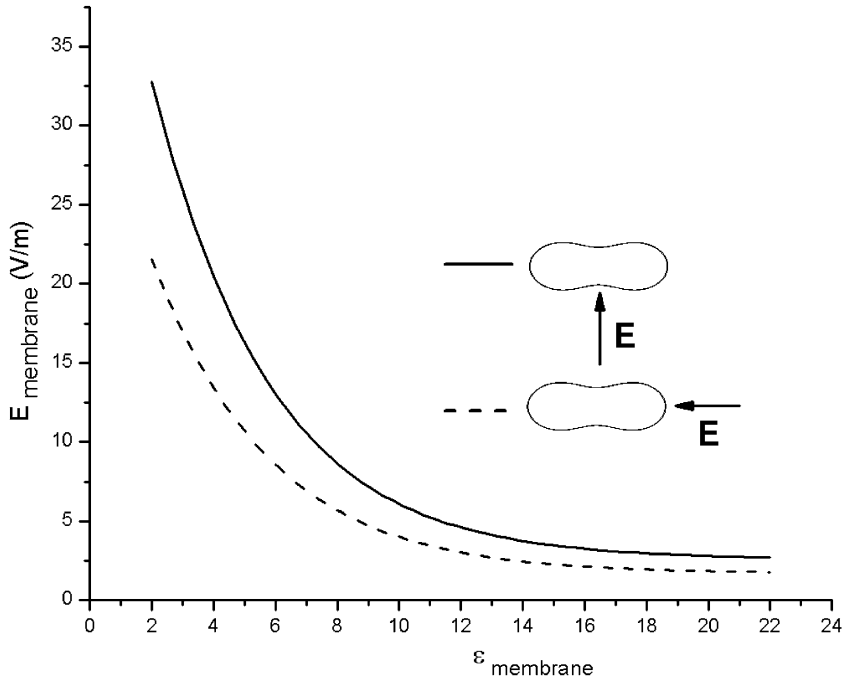

Fig. 2. Electric field distribution within the membrane as a function of the membrane permittivity. *E* is measured along the field direction when the incident field is (a) parallel to the minor axis and (b) parallel to the major axis.

S/m, and for a fixed permittivity value of 50, it was found that the membrane electric field was practically constant for both cell orientations, with a maximum deviation of less than 1%. An explanation of the trends observed in Figs. 2 and 3 is found in the continuity of the normal components of $(\varepsilon - i\sigma/\omega)E$ at the interfaces external medium–membrane and membrane-cytoplasm, required by Maxwell's equations. When both the cytoplasm and membrane conductivities change, the small variation observed in the electric field within the membrane is essentially due to the negligible value of the loss tangent at the working frequency. Again, higher electric field values are observed when the orienta-

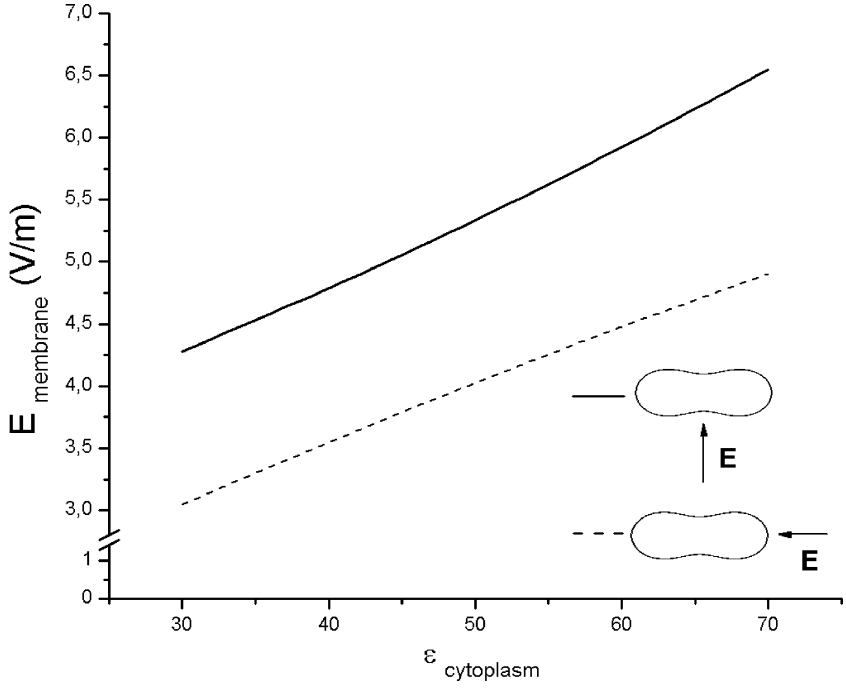

Fig. 3. Electric field distribution within the membrane as a function of the cytoplasm permittivity. *E* is measured along the field direction when the incident field is (a) parallel to the minor axis and (b) parallel to the major axis.

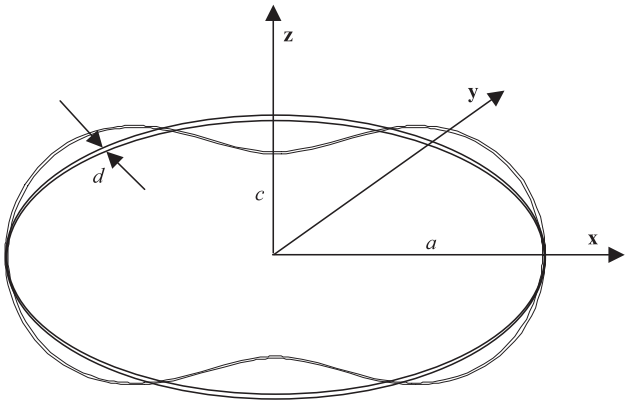

Fig. 4. Oblate spheroid with a confocal layer used to approximate the realistic erythrocyte shape. The oblate spheroid dimensions are $a = c = 3.75$ μm and $b = 2$ μm. The average membrane thickness is $d = 8$ nm, the same as the erythrocyte membrane of Fig. 1.

tion of the external field is parallel to the minor axis of the erythrocyte.

The results of Figs. 2 and 3 show that for a correct analysis of the cell interaction with a MW external field it is necessary to use the proper geometry, the values for the cell electrical properties and its orientation with respect to the incident field. In order to emphasize the former aspect, an oblate spheroid with a confocal layer, a model that is commonly found in literature for modelling an erythrocyte [1,5,6], has been analyzed and the results are compared. Fig. 4 shows the geometry used for the confocal spheroid. The spheroid semiaxes have been chosen as $a = b = 3.75$ μm and $c = 2$ μm, so that it has the same volume as our realistic model (118 μm^3). The values of the membrane thickness along the x and z axes are 5.5 and 10.31 nm, respectively, thus giving an average thickness of 8 nm, equal to the value for the erythrocyte membrane.

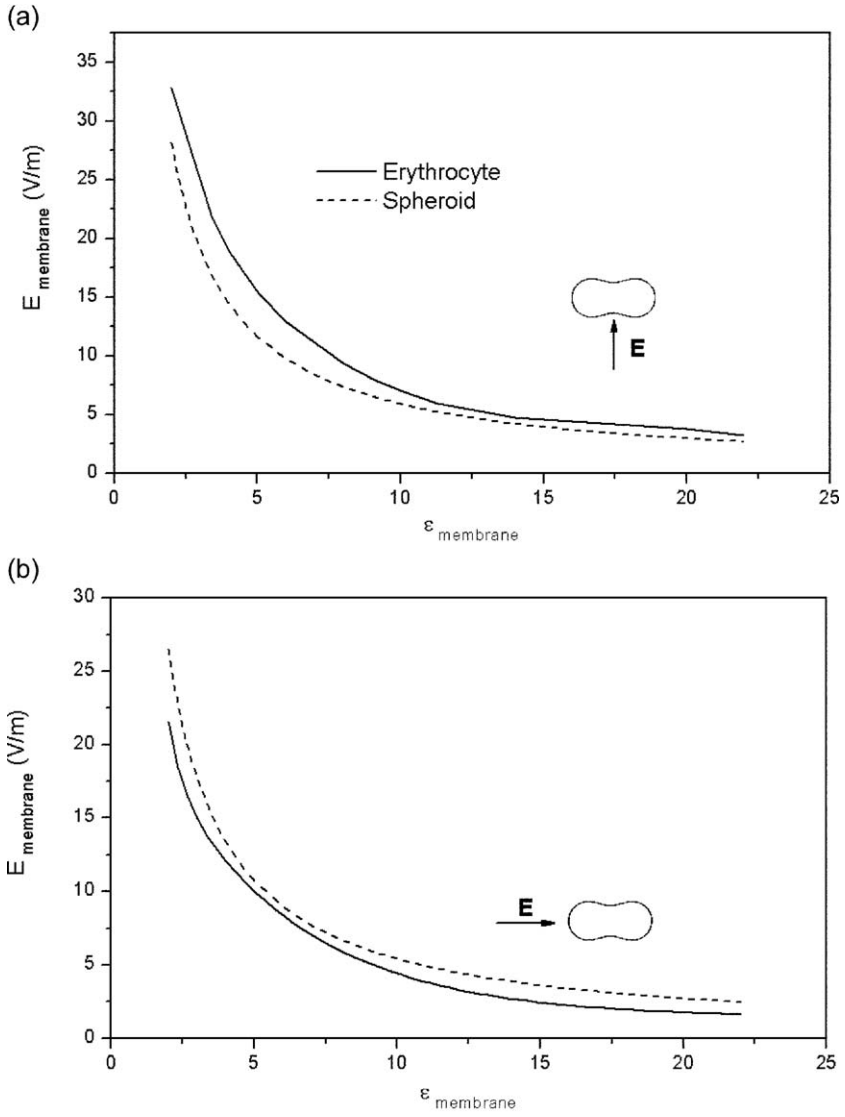

Fig. 5. Electric field intensity within the membrane as a function of its permittivity for the realistic model (erythrocyte) and the confocal oblate spheroid. E is measured along the field direction when the incident field is (a) parallel to the minor axis and (b) parallel to the major axis.

Using the mathematical approach described by Stratton [21], the analytical solution for the field induced in a layered spheroid is found for an external MW applied along the minor and major axes directions. The electric potentials in each of the three regions (cytoplasm, membrane and external medium) are expressed as trial functions which are solutions of Laplace's equation, using ellipsoidal coordinates (ξ, η, ζ). Once the potentials have been calculated, the fields at the cytoplasm, membrane and external medium are readily available.

The last two columns of Table 1 show the values of the electric field within the membrane and cytoplasm of the spheroid using the same electrical parameters of the erythrocyte. Fig. 5a and b shows a comparison of the results obtained using our numerical approach and the analytical solution for the spheroidal model, when the membrane permittivity is varied from 2 to 22 and the external MW field applied is parallel to the minor and major axes, respectively. When E field is parallel to the minor axis, the field amplification factor is higher for the Cassini geometry than for the spheroidal model. The difference between both models becomes less significant as the membrane permittivity value increases. However, when the cell is oriented so that its major axis is parallel to the applied field, the field amplification factor for the erythrocyte is lower than the one for the spheroid and the difference between both models is practically constant.

Similarly, Fig. 6a and b shows the field intensities found within the membrane of the erythrocyte and spheroid as a function of the cytoplasm permittivity for both orientations of the cell. It is observed that the field values obtained are significantly different for the whole range of variation of

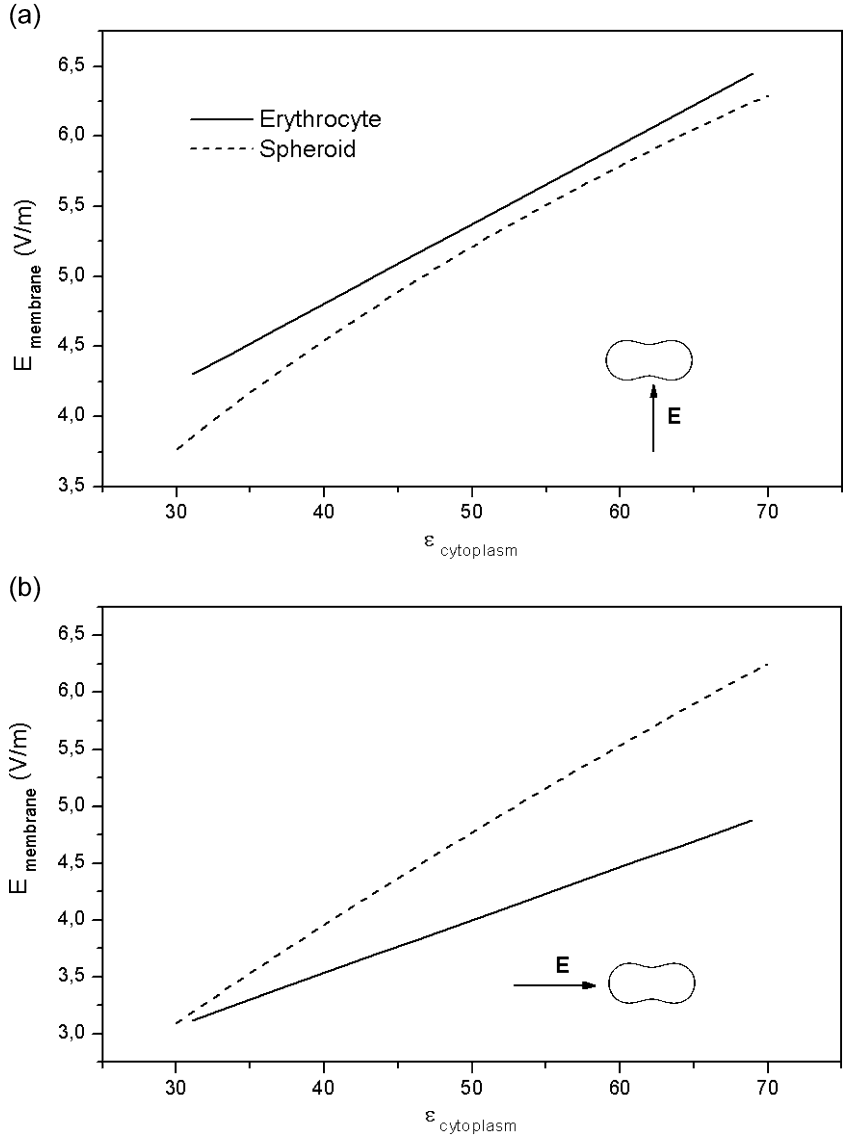

Fig. 6. Electric field intensity within the membrane as a function of the cytoplasm permittivity for the realistic model (erythrocyte) and the confocal oblate spheroid. E is measured along the field direction when the incident field is (a) parallel to the minor axis and (b) parallel to the major axis.

$\varepsilon_{cytoplasm}$ (30 to 70) and again, the biggest discrepancy is found when the external applied field is parallel to the major axis. In this case, the differences between both models are more significant than those shown in Fig. 5a and b for the membrane permittivity variation.

5. Conclusions

The basic goal of the research described in this article has been to analyze the polarization behaviour of erythrocytes exposed to an external MW field. To this end, we have used an accurate FE computational approach with adaptive meshing and improved boundary conditions, and have studied the influence of the modelling parameters on the induced field at the cell membrane, as a possible target of harmful effects of field exposure. The results presented above clearly show the influence of the assumed electrical properties and orientation of the cell on the internal electric field distribution. Depending on the membrane permittivity value, the amplification factor in the electric field from the external medium to the membrane can vary from 5 to 30. The coupling from the air to the tissues reduces the field radiated by an antenna by a factor of about 100. This fact and the high value of the natural transmembrane field (of the order of 10^7 V m^{-1}) have produced a lot of controversy about the possible carcinogenic or other health effects of weak EMF. However, there is a growing database of reported effects and these call for the need of accurate theoretical and experimental determination of the electrical response of cells.

Analytical methods provide useful estimative calculations but contain unrealistic assumptions such as non-uniformity of the membrane thickness or too simplistic geometry. The comparison of our results with other values previously published for spheres and spheroids shows the importance of using a realistic shape for modelling a cell, at the expense of mathematical complexity and computing time. As it has been shown, many studies which have used confocal spheroids as a model for erythrocytes are rough approximations if a precise simulation of the bioeffects in cells is desired.

References

[1] J. Gimsa, D. Wachner, On the analytical description of the transmembrane voltage induced on spheroidal cells with zero membrane conductance, Eur. Biophys J. 30 (2001) 463–466.
[2] J.C. Lin, A.W. Guy, C.C. Johnson, Power deposition in a spherical model of man exposed to 1–20 MHz electromagnetic fields, IEEE Trans. Microwave Theor. Tech. 23 (1975) 246–253.
[3] L.M. Liu, S.F. Cleary, Absorbed energy distribution from radiofrequency electromagnetic radiation in mammalian cell model: effect of membrane-bound water, Bioelectromagnetics 16 (1995) 160–171.
[4] P. Bernardi, M. Cavagnaro, G. D'Inzeo, M. Liberti, Cell modeling to evaluate EM field absorption in biological samples, Proc. URSI XXVI General Assembly, Toronto, N.A. Sarault, National Research Council, Canada, 1999, p. 616.
[5] J. Gimsa, D. Wachner, Analytical description of the transmembrane voltage induced on arbitrarily oriented ellipsoidal an cylindrical cells, Biophys. J. 81 (2001) 1888–1896.
[6] J.L. Sebastian, S. Muñoz San Martin, M. Sancho, J.M. Miranda, Analysis of the influence of the cell geometry orientation and cell proximity effects on the electric field distribution from direct RF exposure, Phys. Med. Biol. 46 (2001) 213–225.
[7] S. Muñoz San Martin, J.L. Sebastian, M. Sancho, J.M. Miranda, A study of the electric field distribution in erythrocyte and rod shape cells from direct RF exposure, Phys. Med. Biol. 48 (2003) 1649–1659.
[8] J. Thuery, in: E.H. Grant (Ed.), Microwaves: Industrial, Scientific and Medical Applications, Artech House, Norwood, MA, 1992, pp. 553–569.
[9] P. Moon, D.E. Spencer, Field Theory Handbook, Springer Verlag, Berlin, 1998.
[10] P. Kuchel, E. Fackerell, Parametric equation representative of biconcave erythrocytes, Bull. Math. Biol. 61 (1999) 209–220.
[11] A. Gray, Modern Differential Geometry of Curves and Surfaces with Mathematica, 2nd ed. CRC Press.
[12] Mathematica version 4.2, Wolfram Research, 2002.
[13] L. Stryer, Biochemistry, 4th ed., Freeman, New York, 1995.
[14] J.P. Huang, K.W. Yu, Dielectric behaviour of oblate spheroidal particles: application to erythrocytes suspensions, Commun. Theor. Phys., (2002) 82–87.
[15] R. Martinsen, S. Grimnes, H. Schwan, Interface phenomena and dielectric properties of biological tissue, Encycl. Surf. Colloid Sci., (2002) 2643–2652.
[16] J.Z. Bao, C.C. Davis, R.E. Schmukler, Frequency domain impedance measurements of erythrocytes. Constant phase angle impedance characteristics and a phase transition, Biophys. J. 61 (1992) 1427–1434.
[17] M. Simeonova, D. Wachner, J. Gimsa, Cellular absorption of electric field energy: the influence of molecular properties of the cytoplasm, Bioelectrochemistry 56 (2002) 215–218.
[18] S. Gabriel, R.W. Lau, C. Gabriel, The dielectric properties of biological tissues: III. Parametric models for the dielectric spectrum of tissues, Phys. Med. Biol. 41 (1996) 2271–2293.
[19] J. Jin, The Finite Element Method in Electromagnetics, Wiley, New York, 1993.
[20] E. Becache, P. Joly, On the analysis of Berenger's perfectly matched layers for Maxwell equations, INRIA Report, vol. 4164, 2001 (Grenoble).
[21] J. Stratton, Electromagnetic Theory, McGraw-Hill, New York, 1941, pp. 513–573.